ISSN 1392–1320 MATERIALS SCIENCE (MEDŽIAGOTYRA). Vol. 29, No. 4. 2023

Structures and Electronic Properties of Titanium Oxo Clusters with Tartrate Ligand: A Density Functional Theory Study

Jing HUANG [1, 2] *, Lei YANG [3], Shasha ZENG [2]

[1] *College of Environmental and Biological Engineering, Putian University, Putian, Fujian 351100, China*
[2] *Fujian Provincial Key Laboratory of Ecology-Toxicological Effects & Control for Emerging Contaminants, Putian, Fujian 351100, China*
[3] *Key Laboratory of Ecological Environment and Information Atlas, Fujian Provincial University, Putian, Fujian 351100, China*

http://dx.doi.org/10.5755/j02.ms.33426

Received 23 February 2023; accepted 11 April 2023

Titanium oxo clusters are considered a model for nanotitanium dioxide and have gradually become a new field of functional materials in solar cells. In this work, the precise structural information of two types of tartrate-based titanium-oxo clusters was investigated by quantum chemical approaches. Density functional theory (DFT) and time-dependent density functional theory (TDDFT) calculations provided the precise structural parameters of $Ti_4(C_4H_2O_6)(AS)_2(O^iPr)_{10}$ and $Ti_4(C_4H_2O_6)(ATS)_2(O^iPr)_{10}$. Our work provided reliable results in agreement with the experimental results. In both molecules, the Ti-O bonds were mainly divided into three categories: the bonds in the first category were the coordination bonds between the central skeleton Ti atom and the tartaric acid group, whose bond lengths were 2.000 – 2.080 Å; the bonds in the second category were the coordination bond formed by the Ti atom and the oxygen on the AS ligand sulphonic acid group, whose bond lengths were 2.148 – 2.310 Å; the bonds in the third category were the Ti-O bonds with shorter bond lengths, which were the coordination bond formed by the Ti atom and the oxygen on the isopropylalkoxy group with their bond lengths in the value range from 1.777 Å to 1.795 Å. These kinds of Ti-O bonds also can be found in other Ti_4 titanium-oxo clusters. Molecular orbitals showed that electron transfer from the AS/ATS ligand to the $\{Ti_4\}$ central skeleton was induced by sunlight with maximum UV-Vis absorption of 605/629 nm. Our calculation results provide strong guidance for the discovery of new efficient titanium oxo in solar cells.
Keywords: titanium-oxo clusters, density functional theory, tartrate-based molecule, Ti-O bond.

1. INTRODUCTION

With the rapid progress of industrial production and the sudden advances of the past hundred years, human life has been radically changed and the quality of people's lives has improved. However, along with progress have come many problems. Today, the development and use of green energy have become an important issue in scientific research due to the over-exploitation of resources, new depletion of global fossil energy sources, threats to natural ecosystems, and increasing environmental pollution [1]. Research and development of clean technologies and environmentally friendly materials are urgently needed to solve energy and environmental problems [2 – 5]. Among the many candidate materials, solar energy is inexhaustible; moreover, at the current level of technological development, solar energy utilisation is not only possible and feasible, but also a purely renewable energy source [6 – 9]. Therefore, photocatalytic materials could utilise clean solar energy to solve related energy and environmental problems and have become a highly attractive research direction.

Among many titanium-based materials, titanium dioxide (TiO_2) has been widely used in various fields as an n-type semiconductor photocatalytic material with outstanding properties such as low cost, safety and non-toxicity, abundant resources, chemical stability and high photocatalytic activity [10 – 14]. Especially in environmental photocatalysis, TiO_2 plays an outstanding role and can be used for the photolysis of pollutants, air and water purification, and self-cleaning and anti-fogging films [15]. In solar energy harvesting, TiO_2 can be used in new energy fields such as hydrogen production from photolysed water and dye-sensitised photovoltaic cells [16, 17]. Titanium dioxide is also an important support for many efficient metal catalysts, which can be loaded with different types of metals involved in different chemical reactions, such as TiO2-loaded Au catalysts for CO oxidation reactions [18]. However, TiO2 itself still had defects, such as a complex surface structure, which made it difficult to establish the relationship between structure and properties, while TiO_2 as a broadband n-type semiconductor material had disadvantages, such as a high band gap value and easy compounding of photogenerated electron holes, as well as the nature that it only received UV light stimulation, which limited its efficiency in the use of sunlight [19 – 21]. The common approach to solve this problem was to functionalise and dope this material to better harness solar energy while maintaining its high efficiency and stability, which would be an important advance in titanium-based photocatalysts [22 – 24]. As a model compound for the structure and reaction of titanium dioxide materials,

* Corresponding author. Tel.: +086-13859875614; fax: +086-2697878.
E-mail address: *jinghuang@ptu.edu.cn* (J. Huang)

crystalline titanium oxo clusters (TOCs) with well-defined structural information have become the focus of attention [25]. With the development of recent single crystal X-ray diffraction. With the advent of technology and structural resolution software, a growing number of researchers have turned their attention to the emerging field of crystalline titanium-oxygen clusters, and a series of advances have been made [26 – 30]. The precise atomic position information, well-defined ligand cluster nucleus linkage, tunable nucleus size and good solubility of titanium-oxygen clusters provided the opportunity to understand their conformational relationships and expand their functional applications and provided an excellent platform for molecular simulations and theoretical calculations of related titanium dioxide surface modifications [31].

Titanium-oxo clusters (TOCs) were usually heteropolymetallic oxides of the type $[Ti_xO_y(OR)_z]$, $[Ti_xO_y(OR)_z(L)_m]$, $[Ti_xO_y(OR)_zM_n]$ or $[Ti_xO_y(OR)_z(L)_mM_n]$ (or OR = alcohol salt, L = functional ligand, M = transition metal or lanthanide ion) [3, 32]. The precise structural information and the solubility in solvents would have the residence patterns of the further application of titanium oxo clusters [3, 32]. In this work, a density functional approach was used to investigate the geometry and electronic structure of two titanium oxo clusters. Two molecules were considered here, $Ti_4(C_4H_2O_6)(AS)_2(O^iPr)_{10}$ (molecule 1) and $Ti_4(C_4H_2O_6)(ATS)_2(O^iPr)_{10}$ (molecule 2) where $(C_4H_2O_6)$ represents the tartaric acid root, AS means aniline-2-sulfonate, and ATS is 4-aminotoluene-3-sulfonate.

2. METHODS

2.1. Conformation optimisation

Gaussian 09 software [33] was used to optimise the geometric configuration of selected molecules. The geometric configuration optimisation process was carried out using the B3LYP [34] heterogeneous density functional theory, which consists of the LYP function, the VWN equation and the Hartree-Fock equation. Previous studies have shown that the B3LYP approaches can provide reliable results for geometric optimisation and quantum calculations of the electronic structure of titanium cluster compounds. More accurate Sddall basis groups and Sddall pseudopotentials were used for Ti atoms, and all-electron 6-31G(d,p) basis groups for the rest of the atoms. The initial structure of molecule 1 was obtained from the Cambridge Crystallographic Data Centre (CCDC) with crystal number 2046547 [32] and the modification of the AS ligand to the ATS ligand resulted in the structure of molecule 2.

2.2. Electron transfer analysis

TDDFT method was used to study the distribution of photoexcitation processes in two titanium oxo clusters. The generalised cam-B3LYP [35] function, combined with B3LYP and Tawada's long-range correction[36], was used for the excited state calculations in the B3LYP-optimised geometries, taking into account the excitation of 20 states. The Sddall basis group and Sddall pseudopotential were used for the Ti atoms, and the all-electron 6-311G++(d,p) basis group was used for the rest of the atoms.

3. RESULTS AND DISCUSSION

3.1. Geometric structure optimisation

3.1.1. $Ti_4(C_4H_2O_6)(AS)_2(O^iPr)_{10}$ cluster

The optimised geometric configuration of the $Ti_4(C_4H_2O_6)(AS)_2(O^iPr)_{10}$ molecule is shown in Fig. 1. The overall spatial arrangement of the molecule is shown in Fig. 1 a. The molecule consisted of four Ti atoms ligated with tartaric acid ligands to form a central framework plane, with each Ti atom having a six-coordinated structure. The six isopropyl oxygens were coordinated to the remaining coordination site on the Ti atom of the central skeleton. For the skeleton centre consisting of Ti atoms and tartaric acid ligands (as shown in Fig. 1 b), the transverse span was 5.962 Å and the longitudinal span was 3.249 Å.

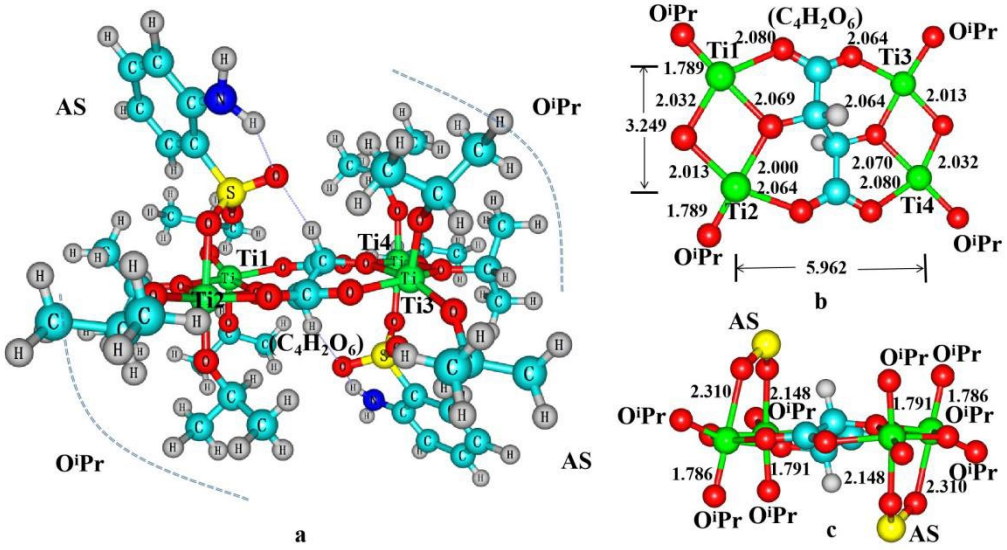

Fig. 1. Optimised geometry of the $Ti_4(C_4H_2O_6)(AS)_2(O^iPr)_{10}$ cluster: a – overall coordination; b – {Ti_4} central skeleton; c – central skeleton (bond lengths in Å in the figure)

The Ti-Ti longitudinal span obtained from the experimental X-ray crystallographic analysis was 3.2194 Å [32]. The theoretical calculation was in good agreement with the experiment. The Ti-O bonds in the structure of molecule 1 were mainly divided into three types: The first type of Ti-O bond was the coordination bond between the central skeletal Ti atom and the tartaric acid group, with a bond length of 2.000 – 2.080 Å (as shown in Fig. 1 b); The second type was the coordination bond formed by the Ti atom and the oxygen on the sulphonic acid group of the AS ligand, whose bond length was 2.148 ~ 2.310 Å. The third type had the short Ti-O atom and a stronger coordination bond, which was the coordination bond formed by the Ti atom and the oxygen on the isopropylalkoxy group with a bond length of 1.777 ~ 1.795 Å (as shown in Fig. 1 b and Fig. 1 c). Similar three types of Ti-O bonds can be also found in other titanium-oxo clusters, such as $Ti_4(O^iPr)_4(L1)_6$ (H_2L1 = salicylaldoxime) [3], $Ti_4(\mu_4\text{-}O)(OMe)_6(L1)_4$ (H_2L1 = salicylaldoxime) [37] and $Ti_4O_2(O^iPr)_8(ON{=}CMe\text{-}CH_2\text{-}CMe{=}NO)_2$ [38].

3.1.2. $Ti_4(C_4H_2O_6)(ATS)_2(O^iPr)_{10}$ molecule

The optimised geometric configuration of the $Ti_4(C_4H_2O_6)(ATS)_2(O^iPr)_{10}$ molecule is shown in Fig. 2. The overall spatial arrangement of the molecule is shown in Fig. 2 a. Similar to the $Ti_4(C_4H_2O_6)(ATS)_2(O^iPr)_{10}$ molecule, the central backbone structure of the $Ti_4(C_4H_2O_6)(ATS)_2(O^iPr)_{10}$ molecule also consists of four Ti atoms ligated with tartaric acid ligands, each Ti atom being a hexa-coordinated structure. Two 4-aminotoluene-3-sulphonic acid (ATS) groups were distributed on opposite sides of the central backbone plane, with two oxygen atoms on each ATS sulphonic acid group coordinated to the Ti atom on the central backbone and the other oxygen atom of the sulphonic acid group forming a hydrogen bond with the nitrogen atom on the ATS ligand.

The six isopropyl oxygens were coordinated to the remaining coordination sites on the Ti atom of the central skeleton. Due to the greater spatial site resistance of the ATS group than the AS group, the Ti-Ti transverse and longitudinal spans of the central backbone of molecule 2 were larger than those of molecule 1. For the molecule 2 central backbone, the Ti-Ti transverse span was 5.943 Å and the longitudinal span was 3.258 Å. The Ti-Ti longitudinal span obtained from the experimental X-ray crystal structure analysis was 3.2323 Å [32]. The theoretical calculation results were in good agreement with the experiment. The Ti-O bond of the molecule 2 structure was 1.777 – 2.220 Å. The Ti-O bond of Ti with tartaric acid was 2.019 ~ 2.068 Å, the Ti-O bond of Ti with ATS group was 2.182 ~ 2.220 Å, and the Ti-O bond of Ti with ATS group was 1.777 ~ 1.801 Å coordinated to the Ti atom on the central backbone and the other oxygen atom of the sulphonic acid group forming a hydrogen bond with the nitrogen atom on the ATS ligand. The six isopropyl oxygens were coordinated to the remaining coordination sites on the Ti atom of the central skeleton. Due to the greater spatial site resistance of the ATS group than the AS group, the Ti-Ti transverse and longitudinal spans of the central backbone of molecule 2 were larger than those of molecule 1. For the molecule 2 central backbone, the Ti-Ti transverse span was 5.943 Å and the longitudinal span was 3.258 Å. The Ti-Ti longitudinal span obtained from the experimental X-ray crystal structure analysis was 3.2323 Å [32], indicating that our calculation was reasonable and the application of the B3LYP method to tartrate-based titanium oxo clusters was reliable. The Ti-O bond of the molecule 2 structure was 1.777 – 2.220 Å. The Ti-O bond of Ti with tartaric acid was 2.019 ~ 2.068 Å, the Ti-O bond of Ti with ATS group was 2.182 ~ 2.220 Å, and the Ti-O bond of Ti with ATS group was 1.777 ~ 1.801 Å.

3.2. Electronic structure analysis

3.2.1. Molecular orbitals of the $Ti_4(C_4H_2O_6)(AS)_2(O^iPr)_{10}$ molecule

The frontier molecular orbitals of $Ti_4(C_4H_2O_6)(AS)_2(O^iPr)_{10}$ are shown in Fig. 3.

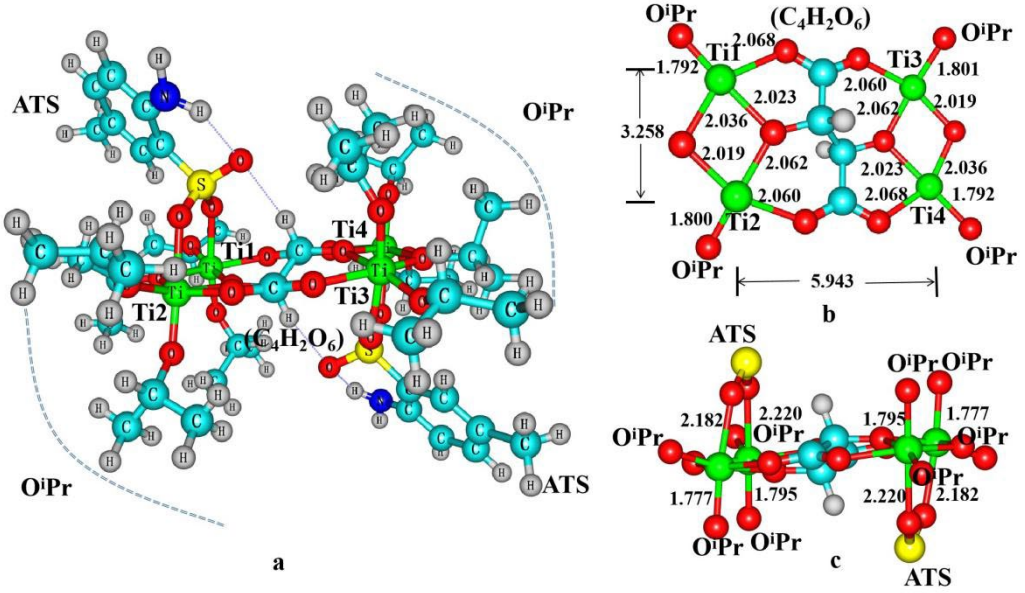

Fig. 2. Optimised geometry of the $Ti_4(C_4H_2O_6)(ATS)_2(O^iPr)_{10}$ molecule: a – overall coordination; b – {Ti_4} central framework; c –central skeleton (bond lengths in Å in the figure)

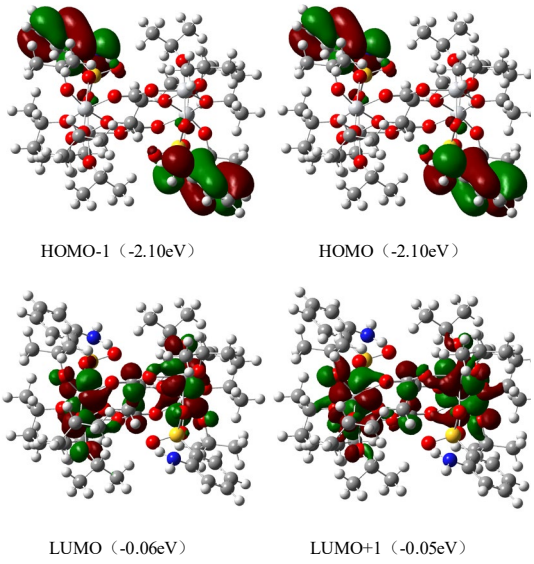

Fig. 3. The TDDFT calculated frontier molecular orbitals of $Ti_4(C_4H_2O_6)(AS)_2(O^iPr)_{10}$ molecule

HOMO was the lowest occupied orbital, and LUMO was the highest unoccupied orbital. The HOMO and HOMO-1 orbitals were the simplicial orbitals with very similar electron cloud shapes, and the electron cloud was concentrated on the benzene ring group on the AS ligand, which was the electron transfer donor. In contrast, the electron cloud of the LUMO and LUMO+1 orbitals was concentrated on the $\{Ti_4\}$ central skeleton, which was mainly composed of a combination of Ti atoms and their coordinated oxygen atoms and tartaric acid ligands. Under photoexcitation, electron leaping from the HOMO (or HOMO-1) to the LUMO (or LUMO+1) can cause the electron cloud to transfer from the benzene ring on AS to the $\{Ti_4\}$ central skeleton. In addition, the intramolecular isopropyl group contributes to the HOMO-1, HOMO, LUMO and LUMO+1 orbitals, as shown in Fig. 3.

3.2.2. Molecular orbitals of the $Ti_4(C_4H_2O_6)(ATS)_2(O^iPr)_{10}$ molecule

The frontier orbitals of $Ti_4(C_4H_2O_6)(ATS)_2(O^iPr)_{10}$ are shown in Fig. 4. Similar to $Ti_4(C_4H_2O_6)(ATS)_2(O^iPr)_{10}$, the HOMO and HOMO-1 orbitals were the simple merger orbitals, the electron cloud was concentrated on the benzene ring group on the ATS ligand, and the ATS ligand was the electron transfer donor. The electron clouds of the LUMO and LUMO+1 orbitals were concentrated on the central skeleton, and the photoexcitation of electrons from the HOMO to LUMO can be regarded as electron transfer from the benzene ring of the ATS ligand to the central skeleton.

3.2.3. Excitation analysis

The TDDFT calculated UV-Vis spectroscopy is shown in Fig. 5. The maximum wavelengths absorbed by molecule 1 and molecule 2 were 605 nm and 629 nm respectively. The absorption wavelengths of the two molecules covered most of the wavelength band of sunlight, in the range of 550 nm to 650 nm for molecule 1 and 600 nm to 700 nm for molecule 2, indicating that these two tartrate-based titanium oxo materials can serve as efficient devices in the solar cell. In addition, the main orbital contribution was derived from the H→L, H-1→L and H-1→L+1 orbitals as shown in Table 1.

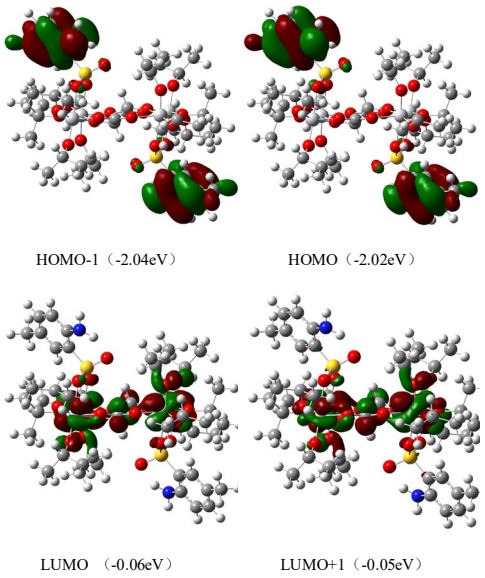

Fig. 4. The TDDFT calculated frontier molecular orbitals of $Ti_4(C_4H_2O_6)(ATS)_2(O^iPr)_{10}$ molecule

In Table 1, the H→L contribution accounted for only ~ 20 % due to the presence of a degenerate energy level between the HOMO and HOMO-1 orbitals.

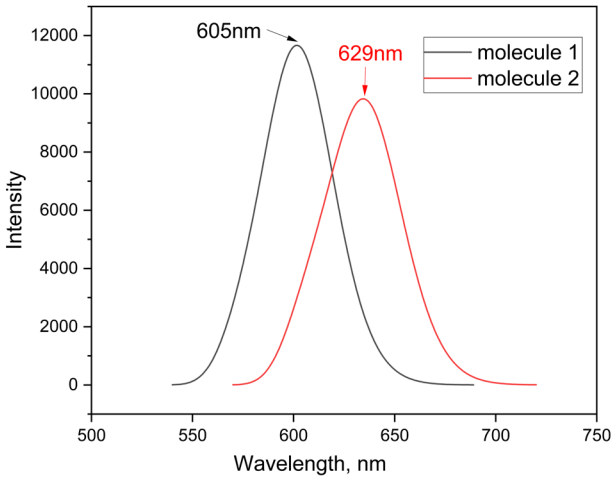

Fig. 5. TDDFT Calculated UV-Vis Spectroscopy

Table 1. The main contribution of the orbitals to the electronic transitions at maximum absorption

Molecules	Orbital contribution
molecule 1	H→L 20.2% H-1→L 31.6% H-1→L+1 28.3%
molecule 2	H→L 19.8% H-1→L 26.7% H-1→L+1 42.5%

4. CONCLUSIONS

In this work, the structure and excitation of two tartrate-based titanium oxo clusters have been investigated by density functional theory. The functionals used in this calculation were reliable, as the optimised geometries of $Ti_4(C_4H_2O_6)(AS)_2(O^iPr)_{10}$ and $Ti_4(C_4H_2O_6)(ATS)_2(O^iPr)_{10}$ were in good agreement with the experimental results.

Molecular orbital analysis indicated that the benzene ring group on the AS/ATS ligand was the electron donor and the {Ti_4} central skeleton was the electron acceptor. The electrons in the AS/ATS ligand were induced by solar energy, followed by electron transfer from the AS/ATS ligand to the {Ti_4} central skeleton. Furthermore, the excitation analysis showed that these two titanium oxo materials could be applied in the solar cell as their absorption wavelengths covered most of the wavelength band of sunlight. Our theoretical investigation would be beneficial for the further development of titanium oxo materials in solar cells.

Acknowledgments

This work was supported by the fund of NSFP of Fujian Province (No.2020J05210, No.2021J011105, No.2022J01132911, No.2022J01132905) Fujian Young and Middle aged Teacher Research Project (JAT220303). Science and Technology correspondent of Fujian Province (202135030079, F2021KTP070). Jing Huang thanks Dr Ayomikunn from the University of Bologna for proofreading.

REFERENCES

1. **Palmer, L.** Green Energy Financing *Nature Sustainability* 5 2022: pp. 910 – 911. https://doi.org/10.1038/s41893-022-00972-y
2. **He, P., Wang, X.X., Cai, Y.Z., Shu, J.C., Zhao, Q.L., Yuan, J., Cao, M.** Tailoring $Ti_3C_2T_x$ Nanosheets to Tune Local Conductive Network as An Environmentally Friendly Material for Highly Efficient Electromagnetic Interference Shielding *Nanoscale* 11 2019: pp. 6080 – 6088.
3. **Wang, C., Chen, N., Kong, F., Wang, S.** A Family of Oxime-based Ttanium-oxo Clusters: Synthesis, Structures, and Photoelectric Responses *CrystEngComm* 24 2022: pp. 3280 – 3286. https://doi.org/10.1039/D2CE00195K
4. **Chen, J., Lü, S., Zhang, Z., Zhao, X., Li, X., Ning, P., Liu, M.** Environmentally Friendly Fertilizers: A Review of Materials Used and Their Effects on the Environment *Science of The Total Environment* 613 – 614 2018: pp. 829 – 839. https://doi.org/10.1016/j.scitotenv.2017.09.186
5. **Emmanuel, I.A., Bernd, W., Klaus, F.** Eco-friendly and Sustainable Processing of Wood-based Materials *Green Chemistry* 23 2021: pp. 2198 – 2232. https://doi.org/10.1039/D0GC04430J
6. **Choi, W., Dong, F., Hatzell, M., Mul, G.** Solar Energy Utilization and Photo(electro)catalysis for Sustainable Environment *ACS EST Engineering* 2 (6) 2022: pp. 940 – 941. https://doi.org/10.1021/acsestengg.2c00182
7. **Zhao, Y., Zhang, L., Liu, Y., Deng, Z., Zhang, R., Zhang, S., He, W., Qiu, Z., Zhao, Z., Tang, B.Z.** AIEgens in Solar Energy Utilization: Advances and Opportunities *Langmuir* 38 (29) 2022: pp. 8719 – 8732. https://doi.org/10.1021/acs.langmuir.2c01036
8. **Bai, H., Liu, H., Chen, X., Hu, R., Li, M., He, W., Du, J., Liu, Z., Qin, A., Lan, J., Kwok, R., Tang, B.** Augmenting Photosynthesis Through Facile AIEgen-chloroplast Conjugation and Efficient Solar Energy Utilization *Materials Horizons* 8 2021: pp. 1433 – 1438. https://doi.org/10.1039/D1MH00012H
9. **Lv, J., Xie, J., Mohamed, A.G.A., Zhang, X., Wang, Y.** Photoelectrochemical Energy Storage Materials: Design Principles and Functional Devices Towards Direct Solar to Electrochemical Energy Storage *Chemical Society Reviews* 51 2022: pp. 1511 – 1528. https://doi.org/10.1039/D1CS00859E
10. **Chen, X., Liu, L., Huang, F.** Black Titanium Dioxide (TiO_2) Nanomaterials *Chemical Society Reviews* 44 2015: pp. 1861 – 1885. https://doi.org/10.1039/C4CS00330F
11. **Hansaraj, D., Varad, K., Amey, D., Sekar, S.K.** Titanium Dioxide as A Photocatalyst to Create Self-cleaning Concrete *Material Today: Proceedings* 45 (4) 2021: pp. 4058 – 4062. https://doi.org/10.1016/j.matpr.2020.10.948
12. **Andrey, A.R., Albina, A.V., Alexander, S.V., Ilya, A.W.** Titanium Dioxide Nanotubes: Synthesis, Structure, Properties and Applications *Russian Chemical Reviews* 90 2021: pp. 1397. https://iopscience.iop.org/article/10.1070/RCR4991
13. **Waghmode, M.S., Gunjal, A.B., Mulla, J.A.** Studies on the Titanium Dioxide Nanoparticles: Biosynthesis, Applications and Remediation *SN Applied Sciences* 1 2019: pp. 310. https://doi.org/10.1007/s42452-019-0337-3
14. **Kang, X., Liu, S., Dai, Z., He, Y., Song, X., Tang, Z.** Titanium Dioxide: From Engineering to Applications *Catalysts* 9 (2) 2019: pp. 191. https://doi.org/10.3390/catal9020191
15. **Chemin, J.B., Bulou, S., Baba, K., Fontaine, C., Sindzingre, T., Boscher, N.D., Choquet, P.** Transparent Anti-fogging and Self-cleaning TiO_2/SiO_2 Thin Films on Polymer Substrates Using Atmospheric Plasma *Scientific Reports* 8 2018: pp. 9603. https://doi.org/10.1038/s41598-018-27526-7
16. **Ge, M., Li, Q., Cao, C., Huang, J., Li, S., Zhang, S., Chen, Z., Zhang, K., Al-Deyab, S.S., Lai, Y.** One-dimensional TiO_2 Nanotube Photocatalysts for Solar Water Splitting *Advanced Science* 4 (1) 2017: pp: 1600152. https://doi.org/10.1002/advs.201600152
17. **Fan, J., Liu, S., Yu, J.** Enhanced Photovoltaic Performance of Dye-sensitized Solar Cells Based on TiO_2 Nanosheets/Graphene Composite Films *Journal of Materials Chemistry* 22 2012: pp. 17027 – 17036. https://doi.org/10.1039/C2JM33104G
18. **Wang, Y.G., Cantu, D.C., Lee, M.S., Li, J., Glezakou, V.A., Rousseau, R.** CO Oxidation on Au/TiO_2: Condition-Dependent Active Sites and Mechanistic Pathways *Journal of the American Chemical Society* 138 (33) 2016: pp. 10467 – 10476. https://doi.org/10.1021/jacs.6b04187
19. **Annita, F., Sonia, L., Brunno, F.S.** Assessment of TiO_2 Band Gap from Structural Parameters Using Artificial Neural Networks *Journal of Photochemistry and Photobiology A: Chemistry* 405 (15) 2021: pp. 112870. https://doi.org/10.1016/j.jphotochem.2020.112870
20. **Dong, H., Zeng, G., Tang, L., Fan, C., Zhang, C., He, X., He, Y.** An Overview on Limitations of TiO_2-based Particles for Photocatalytic Degradation of Organic Pollutants and the Corresponding Countermeasures *Water Research* 79 2015: pp. 128 – 146. https://doi.org/10.1016/j.watres.2015.04.038
21. **Dette, C., Pérez-Osorio, M.A., Kley, C.S., Punke, P., Patrick, C.E., Jacobson, P., Giustino, F., Jung, S.J., Kern, K.** TiO_2 Anatase with A Bandgap in the Visible Region *Nano Letters* 14 (11) 2014: pp: 6533 – 6538. https://doi.org/10.1021/nl503131s

22. **Muhammad, T., Azmat, A.K., Sehar, T., Rehan, M., Wei, K.** Titanium Carbide (Ti_3C_2) MXene as a Promising Co-catalyst for Photocatalytic CO_2 Conversion to Energy-Efficient Fuels: A Review *Energy Fuels* 35 (13) 2021: pp. 10374 – 10404. https://doi.org/10.1021/acs.energyfuels.1c00958
23. **Wu, Z., Li, C., Li, Z., Feng, K., Cai, M., Zhang, D., Wang, S., Chu, M., Zhang, C., Shen, J., Huang, Z., Xiao, Y., Ozin, G.A., Zhang, X., He, L.** Niobium and Titanium Carbides (MXenes) as Superior Photothermal Supports for CO_2 Photocatalysis *ACS Nano* 15 (3) 2021: pp. 5696 – 5705. https://doi.org/10.1021/acsnano.1c00990
24. **Cai, M., Wu, Z., Li, Z.** Greenhouse-inspired Supra-Photothermal CO_2 catalysis *Nature Energy* 6 2021: pp. 807 – 814. https://doi.org/10.1038/s41560-021-00867-w
25. **Laurence, R., Clément, S.** Titanium Oxo-clusters: Precursors for A Lego-like Construction of Nanostructured Hybrid Materials *Chemical Society Reviews* 40 2021: pp. 1006 – 1030. https://doi.org/10.1039/C0CS00137F
26. **Sun, Y., Lu, D., Sun, Y., Cao, M.Y., Zheng, N., Gu, C., Wang, F., Zhang, J.** Large Titanium-Oxo Clusters as Precursors to Synthesize the Single Crystals of Ti-MOFs *ACS Materials Letters* 3 (1) 2021: pp. 64 – 68. https://doi.org/10.1021/acsmaterialslett.0c00456
27. **Fu, M.Y., Wang, H.Y., Zhai, H.L., Zhu, Q.Y., Dai, J.** Assembly of a Titanium-Oxo Cluster and a Bismuth Iodide Cluster, a Single-Source Precursor of A P-N-Type Photocatalyst *Inorganic Chemistry* 60 (13) 2021: pp. 9589 – 9597. https://doi.org/10.1021/acs.inorgchem.1c00816
28. **Cui, Y., Liu, P.F., Li, M.** Structures, Photoelectrochemical and Photocatalytic Properties of Phosphite-Stabilized Titanium-Oxo Clusters Functionalized with Ferrocenecarboxylate Ligands *Journal of Cluster Science* 30 2019: pp. 1519 – 1524. https://doi.org/10.1007/s10876-019-01595-8
29. **Li, X., Zhu, Y., Gai, Y., Shi, Y., Wei, T., Wang, Y., Zhou, A., Zhang, H., Wang, H., Xiong, K.** Syntheses, Crystal Structures and Photocatalytic Properties of Homometallic and Heterometallic Titanium-oxo Clusters *Inorganic Chemistry Communications* 123 2021: pp. 108324. https://doi.org/10.1016/j.inoche.2020.108324
30. **Wu, Y.X., Liu, X.R., Chen, G., Tian, Y.Q., Yan, J., Yi, X., Liu, X.** Cd-Doped Polyoxotitanium Nanoclusters with A Modifiable Organic Shell for Photoelectrochemical Water Splitting *Inorganic Chemistry* 60 (24) 2021: pp. 19263 – 19269. https://doi.org/10.1021/acs.inorgchem.1c03078
31. **Fan, X., Wang, J., Wu, K., Zhang, L., Zhang, J.** Isomerism in Titanium-Oxo Clusters: Molecular Anatase Model with Atomic Structure and Improved Photocatalytic Activity *Angewandte Chemie (International ed. in English)* 58 (5) 2019: pp. 1320 – 1323. https://doi.org/10.1002/anie.201809961
32. **Mou, W.Y., Xie, B., Li, X.L., Lai, C., Li, T., Chen, L., Feng, J., Bai, X., Wu, Y., Wu, W., Zhang, D., Gu, Y.** Tartrate-stabilized Titanium-oxo Clusters Containing Sulfonate Chromophore Ligands: Synthesis, Crystal Structures and Photochemical Properties *New Journal of Chemistry* 45 2021: pp. 10930 – 10939. https://doi.org/10.1039/D1NJ01540K
33. **Frisch, M.J., Trucks, G.W., Schlegel, H.B., Scuseria, G.E., Robb, M.A., Cheeseman, J.R., Scalmani, G., Barone, V., Petersson, G.A., Nakatsuji, H., Li, X., Caricato, M., Marenich, A., Martin, R.L., Morokuma, K., Farkas, O., Foresman, J.B., Fox, D.J.** Gaussian 09, Revision E.01. 2009. http://gaussian.com
34. **Tirado-Rives, J., Jorgensen, W.L.** Performance of B3LYP Density Functional Methods for A Large Set of Organic Molecules *Journal of Chemical Theory and Computation* 4 2008: pp. 297 – 306. https://doi.org/10.1021/ct700248k
35. **Yanai, T., Tew, D., Handy, N.** A New Hybrid Exchange-Correlation Functional Using the Coulomb-attenuating Method (CAM-B3LYP) *Chemical Physics Letters* 393 2004: pp. 51 – 57. https://doi.org/10.1016/j.cplett.2004.06.011
36. **Tawada, Y., Tsuneda, T., Yanagisawa, S., Yanai, T., Hirao, K.** A Long-range-corrected Time-dependent Density Functional Theory *The Journal of Chemical Physics* 120 2004: pp. 8425 – 8433. https://doi.org/10.1063/1.1688752.
37. **Chen, S., Fang, W.H., Zhang, L., Zhang, J.** Synthesis, Structures, and Photocurrent Responses of Polyoxo-Titanium Clusters with Oxime Ligands: From Ti_4 to Ti_{18} *Inorganic Chemistry* 57 (15) 2018: pp. 8850 – 8856. https://doi.org/10.1021/acs.inorgchem.8b00751
38. **Baumann, S.O., Bendova, M., Fric, H., Puchberger, M., Visinescu, C., Schubert, U.** Ketoximate Derivatives of Titanium Alkoxides and Partial Hydrolysis Products Thereof *European Journal of Inorganic Chemistry* 2009 2009: pp. 3333 – 3340. https://doi.org/10.1002/ejic.200900381.

© Huang et al. *2023* Open Access This article is distributed under the terms of the Creative Commons Attribution 4.0 International License (http://creativecommons.org/licenses/by/4.0/), which permits unrestricted use, distribution, and reproduction in any medium, provided you give appropriate credit to the original author(s) and the source, provide a link to the Creative Commons license, and indicate if changes were made.